Chemistry of Polynuclear Metal Complexes with Bridging Carbene or Carbyne Ligands. Part 68.[1] Reactions Between Nonacarbonyldi-iron and the Salts $[NEt_4][W(\equiv CR)(CO)_2(\eta^5\text{-}C_2B_9H_9Me_2)]$ (R = Me, Ph, or C_6H_4Me-4); Crystal Structures of $[NEt_4][FeW\{\mu\text{-}CH(C_6H_4Me\text{-}4)\}(\mu\text{-}\sigma:\eta^5\text{-}C_2B_9H_8Me_2)(\mu\text{-}CO)(CO)_5]$ and $[NEt_4][Fe_2W(\mu_3\text{-}CPh)(\mu\text{-}\sigma:\sigma',\eta^5\text{-}C_2B_9H_7Me_2)(CO)_8]$ *

Franz-Erich Baumann, Judith A. K. Howard, Owen Johnson, and F. Gordon A. Stone
Department of Inorganic Chemistry, The University, Bristol BS8 1TS

Treatment of the compound $[NEt_4][W(\equiv CMe)(CO)_2(\eta^5\text{-}C_2B_9H_9Me_2)]$ with $[Fe_2(CO)_9]$ in tetrahydrofuran at room temperature affords the trimetal compound $[NEt_4][Fe_2W(\mu_3\text{-}CMe)(\mu\text{-}\sigma:\sigma',\eta^5\text{-}C_2B_9H_7Me_2)(CO)_8]$. Similar reactions between $[Fe_2(CO)_9]$ and the salts $[NEt_4][W(\equiv CR)(CO)_2(\eta^5\text{-}C_2B_9H_9Me_2)]$ (R = Ph or C_6H_4Me-4) afford mixtures of the di- and tri-metal compounds $[NEt_4][FeW\{\mu\text{-}CH(R)\}(\mu\text{-}\sigma:\eta^5\text{-}C_2B_9H_8Me_2)(\mu\text{-}CO)(CO)_5]$ and $[NEt_4][Fe_2W(\mu_3\text{-}CR)(\mu\text{-}\sigma:\sigma',\eta^5\text{-}C_2B_9H_7Me_2)(CO)_8]$. The structures of the two species $[NEt_4][FeW\{\mu\text{-}CH(C_6H_4Me\text{-}4)\}(\mu\text{-}\sigma:\eta^5\text{-}C_2B_9H_8Me_2)(\mu\text{-}CO)(CO)_5]$ and $[NEt_4][Fe_2W(\mu_3\text{-}CPh)(\mu\text{-}\sigma:\sigma',\eta^5\text{-}C_2B_9H_7Me_2)(CO)_8]$ have been established by *X*-ray diffraction. In the anion of the former, the Fe–W bond [2.625(1) Å] is spanned by an alkylidene group $C(H)C_6H_4Me$-4 [μ-C–Fe 2.153(5), μ-C–W 2.172(5) Å], and a carbonyl ligand [μ-C(O)–Fe 2.021(4), μ-C(O)–W 2.172(5) Å; W–C–O 149.3(3), Fe–C–O 133.2(3)°]. The tungsten atom carries two terminally bound CO groups, and is η^5-co-ordinated by the *nido* face of the carbaborane cage. The latter is linked to the iron *via* a σ bond involving a boron atom adjacent to a carbon atom in the face of the cage. The iron is ligated by three terminally bonded CO groups. In the di-irontungsten salt there is an isosceles triangle of metal atoms [Fe–W 2.645(2), Fe–Fe 2.578(2) Å], capped on one side by the phenylmethylidyne group [μ_3-C–Fe 2.06(1), μ_3-C–W 2.029(8) Å]. On the opposite side of the triangle a $\mu_3\text{-}C_2B_9H_7Me_2$ ligand is η^5-co-ordinated to tungsten with two adjacent boron atoms in the *nido* face of the carbaborane cage forming σ bonds to the iron atoms [Fe–B 2.12(1) and 2.14(1) Å]. There are eight terminally bound carbonyl groups, three attached to each iron atom, and two bonded to the tungsten atom. Treatment of $[NEt_4][Fe_2W(\mu_3\text{-}CMe)(\mu\text{-}\sigma:\sigma',\eta^5\text{-}C_2B_9H_7Me_2)(CO)_8]$ in tetrahydrofuran with $[AuCl(PPh_3)]$, in the presence of $TlPF_6$, affords a tetranuclear metal cluster complex $[AuFe_2W(\mu_3\text{-}CMe)(\mu\text{-}\sigma:\sigma',\eta^5\text{-}C_2B_9H_7Me_2)(CO)_8(PPh_3)]$. The n.m.r. data ($^1H$, ^{13}C-{^1H}, and ^{11}B-{^1H}) for the new compounds are reported and discussed.

The salts $[X][W(\equiv CR)(CO)_2(\eta^5\text{-}C_2B_9H_9Me_2)]$ [**1**, R = Me, Ph, or C_6H_4Me-4; X = NEt_4, $N(PPh_3)_2$, $P(CH_2Ph)Ph_3$, or PPh_4] are becoming useful reagents for preparing dimetal compounds with bridging alkylidyne groups. Thus the complexes $[AuCl(PPh_3)]$, $[RhCl(PPh_3)_3]$, and $[Pt(cod)_2]$ (cod = cyclo-octa-1,5-diene) react with the species (**1**, R = C_6H_4Me-4) to give $[AuW(\mu\text{-}CC_6H_4Me\text{-}4)(CO)_2(PPh_3)(\eta^5\text{-}C_2B_9H_9Me_2)]$ (**2**), $[RhW(\mu\text{-}CC_6H_4Me\text{-}4)(CO)_2(PPh_3)_2(\eta^5\text{-}C_2B_9H_9Me_2)]$ (**3**), and $[P(CH_2Ph)Ph_3][PtW(\mu\text{-}CC_6H_4Me\text{-}4)(CO)_2(cod)(\eta^5\text{-}C_2B_9H_9Me_2)]$ (**4**), respectively.[1,2] In these products the carbaborane group ligates the tungsten atom in the usual pentahapto manner, and is associated with this metal centre only. However, an intriguing feature of several of the reactions designed to afford dimetal compounds has been the observation of a 'non-spectator' role played by the carbaborane ligand. Thus treatment of (**1d**) with the salts $[Ru(CO)(NCMe)_2(\eta\text{-}C_5H_5)][BF_4]$ and $[M(CO)_2(NCMe)_2(\eta^5\text{-}C_9H_7)][BF_4]$ (M = Mo or W, C_9H_7 = indenyl) yields the compounds $[RuW(\mu\text{-}CC_6H_4Me\text{-}4)(CO)_3(\eta^5\text{-}C_5H_5)(\eta^5\text{-}C_2B_9H_9Me_2)]$ (**5**)[3] and $[MW(\mu\text{-}CC_6H_4Me\text{-}4)(CO)_3(\eta^5\text{-}C_9H_7)(\eta^5\text{-}C_2B_9H_9Me_2)]$ (**6**),[4] respectively. In these species the metal–metal bonds are bridged not only by *p*-tolylmethylidyne groups, but also by an *exo*-polyhedral

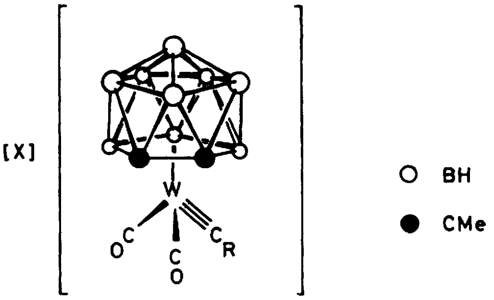

	X	R
(**1a**)	NEt_4	Me
(**1b**)	NEt_4	Ph
(**1c**)	NEt_4	C_6H_4Me-4
(**1d**)	$N(PPh_3)_2$	C_6H_4Me-4
(**1e**)	$P(CH_2Ph)Ph_3$	C_6H_4Me-4
(**1f**)	PPh_4	C_6H_4Me-4

---

* Tetraethylammonium μ-carbonyl-1,1,1,2,2-pentacarbonyl-μ-[7′—11′-η-octahydro-7′,8′-dimethyl-7′,8′-dicarba-*nido*-undecaborato(2 –)-$C^{7',8'}$,$B^{9'-11'}$(W),$B^{9'}$(Fe)]-μ-(*p*-tolylmethylidene)-irontungstate (*Fe–W*) and tetraethylammonium 1,1,1,2,2,2,3,3-octacarbonyl-μ_3-[7′—11′-η-heptahydro-7′,8′-dimethyl-7′,8′-dicarba-*nido*-undecaborato(3 –)-$C^{7',8'}$,-$B^{9'-11'}$ (W),$B^{9'}$(Fe^1),$B^{10'}$(Fe^2)]-μ_3-phenylmethylidyne-*triangulo*-di-irontungstate respectively.

Supplementary data available: see Instructions for Authors, *J. Chem. Soc., Dalton Trans.*, 1987, Issue 1, pp. xvii—xx.

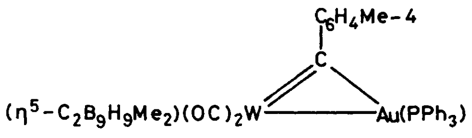

$(\eta^5\text{-}C_2B_9H_9Me_2)(OC)_2W{=}C(C_6H_4Me\text{-}4){-}Au(PPh_3)$

(2)

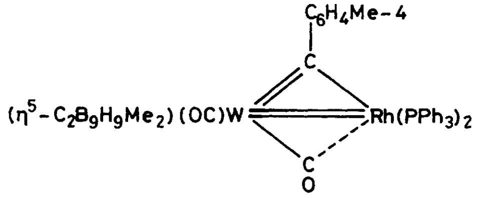

$(\eta^5\text{-}C_2B_9H_9Me_2)(OC)W(\mu\text{-}C C_6H_4Me\text{-}4)(\mu\text{-}CO)Rh(PPh_3)_2$

(3)

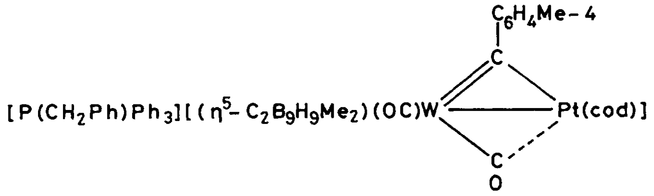

$[P(CH_2Ph)Ph_3][(\eta^5\text{-}C_2B_9H_9Me_2)(OC)W(\mu\text{-}C C_6H_4Me\text{-}4)(\mu\text{-}CO)Pt(cod)]$

(4)

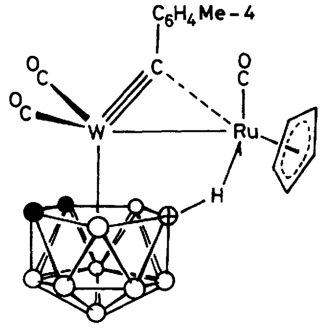

(5)

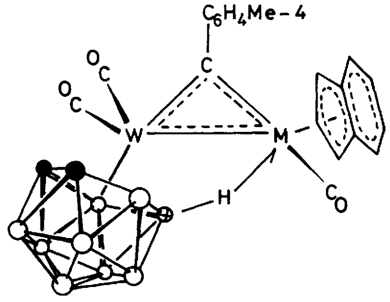

	M
(6a)	Mo
(6b)	W

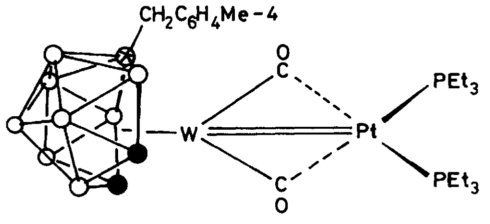

(7)

⊕ B ○ BH ● CMe

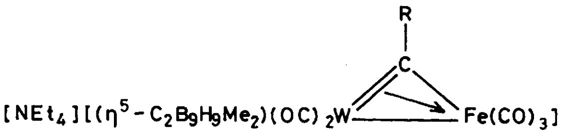

$[NEt_4][(\eta^5\text{-}C_2B_9H_9Me_2)(OC)_2W(\mu\text{-}CR)Fe(CO)_3]$

(**9**, R = Me, Ph, or C_6H_4Me-4)

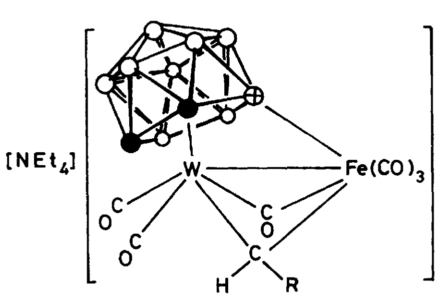

	R
(10a)	Ph
(10b)	C_6H_4Me-4

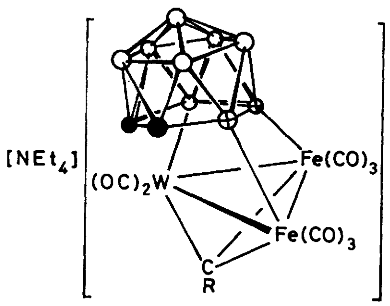

	R
(11a)	Me
(11b)	Ph
(11c)	C_6H_4Me-4

three-centre two-electron B–H $\rightharpoonup$ M (M = Ru, Mo, or W) bond, the latter involving a boron atom in the pentagonal face of the carbaborane ligand. A more substantial involvement of the carbaborane ligand occurs in the reaction between **(1d)** and $[PtH(Me_2CO)(PEt_3)_2][BF_4]$ which affords $[PtW(CO)_2(PEt_3)_2\{\eta^6\text{-}C_2B_9H_8(CH_2C_6H_4Me\text{-}4)Me_2\}]$ **(7)**; in this species the tungsten is ligated by six atoms of the cage, a facial boron atom of which carries a $CH_2C_6H_4Me$-4 substituent derived from the *p*-tolylmethylidyne group.[5]

In view of the unexpected products obtained from several of the reactions studied so far, we have treated the salts (1, R = C_6H_4Me-4) with $[Fe_2(CO)_9]$. Earlier we have shown[6] that the compounds $[W(\equiv CC_6H_4Me\text{-}4)(CO)_2L]$ (L = η-C_5H_5 or η-C_5Me_5), isolobal with the anions in the salts (1), react with $[Fe_2(CO)_9]$ to give dimetal complexes $[FeW(\equiv CC_6H_4Me\text{-}4)(CO)_nL]$ (**8**, *n* = 5 or 6). It might be anticipated, therefore, that the initial products of the reactions between **(1a)**—**(1c)** and $[Fe_2(CO)_9]$ would be the salts $[NEt_4][FeW(\mu\text{-}CR)(CO)_5(\eta^5\text{-}C_2B_9H_9Me_2)]$ (**9**, R = Me, Ph, or C_6H_4Me-4) or related saturated species containing an $Fe(CO)_4$ fragment rather than an $Fe(CO)_3$ group. In practice, although the complexes **(9)** may be initially formed, further transformations involving the carbaborane ligand and other carbonyl–iron groups ensue.

Results and Discussion

Reactions between **(1a)**—**(1c)** and $[Fe_2(CO)_9]$ occur at room temperature in tetrahydrofuran (thf) as solvent over a period of several hours. Column chromatography on alumina of the mixtures obtained revealed that all three reactions afforded the tri-iron compounds $[Fe_3(CO)_{12}]$ and $[NEt_4][Fe_3(\mu\text{-}H)(CO)_{11}]$ as by-products. The products of interest, however, were the di- and tri-metal compounds $[NEt_4][FeW\{\mu\text{-}CH(R)\}(\mu\text{-}\sigma{:}\eta^5\text{-}C_2B_9H_8Me_2)(\mu\text{-}CO)(CO)_5]$ (**10a**, R = Ph; **10b**, R = C_6H_4Me-4) and $[NEt_4][Fe_2W(\mu_3\text{-}CR)(\mu\text{-}\sigma{:}\sigma',\eta^5\text{-}C_2B_9H_7Me_2)(CO)_8]$ (**11a**, R = Me; **11b**, R = Ph; **11c**, R = C_6H_4Me-4). In the reaction between **(1a)** and $[Fe_2(CO)_9]$ a dimetal compound analogous to **(10a)** and **(10b)**, but with a bridging ethylidene ligand, was not observed. Moreover, in the reactions using **(1b)** and **(1c)**, the trimetal compounds **(11)** were the major products (*ca.* 85—95%). Separation of the latter from the dimetal complexes was not complete using column chromatography or fractional crystallisation, and hence this was accomplished by hand picking of crystals, which was not difficult due to different colours and crystal forms.

Data characterising the various compounds **(10)** and **(11)** are given in Tables 1 and 2. However, the structures of these complexes were not established until *X*-ray crystallographic studies had been carried out on **(10b)** and **(11b)**. The results for **(10b)** are summarised in Table 3 and the structure of the anion is shown in Figure 1.

The Fe–W bond [2.625(1) Å] is bridged by a carbonyl ligand [W–C(4)–O(4) 149.3(3), Fe–C(4)–O(4) 133.2(3)°] and by a $CH(C_6H_4Me\text{-}4)$ group [C(7)–Fe 2.153(5), C(7)–W 2.172(5) Å]. The carbaborane group also adopts a bridging mode, being η^5-co-ordinated to the tungsten while also forming a σ bond to the iron *via* B(5) [2.137(6) Å]. The slip distance (Δ) of the tungsten atom in the direction towards the unique boron atom B(5) is 0.26 Å, while the fold angles θ and φ between the perpendicular through the centroid of the B(6)B(7)B(8)B(9)-B(10) ring and the planes defined by B(1)B(2)C(31)C(41) and by B(1)B(5)C(41) are 1.8 and 2.3°, respectively.[7]

The bonding mode of the carbaborane ligand in **(10b)** is similar to that observed previously in the compounds $[N(PPh_3)_2][RuW(\mu\text{-}CC_6H_4Me\text{-}4)(\mu\text{-}\sigma{:}\eta^5\text{-}C_2B_9H_8Me_2)(CO)_3(\eta\text{-}C_5H_5)]$ **(12)**[4] and $[PtW(\mu\text{-}H)\{\mu\text{-}\sigma{:}\eta^5\text{-}C_2B_9H_7(CH_2C_6H_4Me\text{-}4)Me_2\}(CO)_2(PEt_3)_2(PMe_3)]$ **(13)**.[5] There is, however, a subtle difference between the bonding mode of the $\sigma{:}\eta^5$-C_2B_9 group in **(10b)** and **(13)**, compared with that in **(12)**. In the latter the metal(Ru)–boron σ bond is to the central boron of the C_2B_3 face of the icosahedral fragment, whereas in **(10b)** and **(13)** the metal(Fe or Pt)–boron σ bond is to a boron atom adjacent to a CMe group. For **(13)**, a connectivity between the platinum atom and the central boron of the C_2B_3 ring is not possible, since this boron carries a $CH_2C_6H_4Me$-4 substituent. In **(10b)**, the iron atom might have formed a σ bond with B(1) or either of the boron atoms adjacent to the carbons in the face of the cage

Table 1. Analytical[a] and physical data for the iron–tungsten complexes

Compound	Colour	$\nu_{max.}(CO)^b$/cm^{-1}	Analysis (%)		
			C	H	N
(10a) $[NEt_4][FeW\{\mu\text{-}CH(Ph)\}(\mu\text{-}\sigma{:}\eta^5\text{-}C_2B_9H_8Me_2)(\mu\text{-}CO)(CO)_5]$	Red	2 032s, 1 977 (sh), 1 964vs, 1 954s, 1 892m, 1 754w br	38.0 (38.1)	4.9 (5.8)	1.7 (1.8)
(10b) $[NEt_4][FeW\{\mu\text{-}CH(C_6H_4Me\text{-}4)\}(\mu\text{-}\sigma{:}\eta^5\text{-}C_2B_9H_8Me_2)(\mu\text{-}CO)(CO)_5]$	Red	2 031m, 1 971 (sh), 1 963vs, 1 952s, 1 891m, 1 755w br	37.9 (38.1)	4.8 (5.3)	1.5 (1.8)
(11a) $[NEt_4][Fe_2W(\mu_3\text{-}CMe)(\mu\text{-}\sigma{:}\sigma',\eta^5\text{-}C_2B_9H_7Me_2)(CO)_8]$	Black	2 026m, 1 982vs, 1 970s, 1 955m, 1 937w, 1 928 (sh), 1 896w	29.1 (31.6)	4.3 (4.4)	1.7 (1.7)
(11b) $[NEt_4][Fe_2W(\mu_3\text{-}CPh)(\mu\text{-}\sigma{:}\sigma',\eta^5\text{-}C_2B_9H_7Me_2)(CO)_8]$	Black	2 030m, 1 986vs, 1 976s, 1 960m, 1 946w, 1 931w, 1 924 (sh), 1 903w	36.0 (36.1)	4.2 (4.3)	1.7 (1.6)
(11c) $[NEt_4][Fe_2W(\mu_3\text{-}CC_6H_4Me\text{-}4)(\mu\text{-}\sigma{:}\sigma',\eta^5\text{-}C_2B_9H_7Me_2)(CO)_8]$	Black	2 029s, 1 985vs, 1 976s, 1 959s, 1 946m, 1 931m, 1 925 (sh), 1 902w	36.4 (36.9)	4.5 (4.4)	1.4 (1.5)
(15) $[AuFe_2W(\mu_3\text{-}CMe)(\mu\text{-}\sigma{:}\sigma',\eta^5\text{-}C_2B_9H_7Me_2)(CO)_8(PPh_3)]$	Black	[c] 2 042s, 2 013vs, 1 997vs, 1 978w, 1 947m, 1 929m	32.2 (33.0)	2.8 (2.7)	

[a] Calculated values are given in parentheses. [b] In thf; a broad band due to B–H is observed at *ca.* 2 555 cm^{-1}. [c] In Et_2O.

Table 2. Hydrogen-1, carbon-13, and boron-11 n.m.r. data[a] for the iron–tungsten complexes

Compound	$^1H^{b,c}$ (δ)	$^{13}C^{d}$ (δ)	$^{11}B^{e}$ (δ)
(10a)	1.26 (m, 12 H, NCH$_2$*Me*), 2.13 (s, 3 H, CMe), 2.26 (s, 3 H, CMe), 3.09 [q, 8 H, *J*(HH) 8, NC*H*$_2$Me], 6.67 [s br, 1 H, C*H*(Ph)], 6.95 (m, 2 H, Ph), 7.12 (m, 3 H, Ph)	233.7 [WCO, *J*(WC) 134], 213.6 (FeCO), 156.8 [C^1 (Ph)], 129.7—125.2 (Ph), 119.8 [*C*H(Ph), *J*(WC) 46], 66.8, 63.6 (*C*Me), 31.5, 31.3 (C*Me*), 7.7 (NCH$_2$*Me*)	40.7 (1 B, FeB), 6.17 (1 B), 1.41 (1 B), −2.7 to −15.0 (m br, 6 B)
(10b)	1.23 (m, 12 H, NCH$_2$*Me*), 2.12, 2.24, 2.25 (s × 3, 9 H, CMe and Me-4), 3.04 [q, 8 H, *J*(HH) 8, NC*H*$_2$Me], 6.39 [s br, 1 H, C*H*(C$_6$H$_4$Me-4)], 6.83 (m, 4 H, C$_6$H$_4$)	232.3 (WCO), 212.0 (FeCO), 152.1 [C^1 (C$_6$H$_4$)], 128.2—125.3 (C$_6$H$_4$), 119.3 [*C*H(C$_6$H$_4$Me-4), *J*(WC) 48], 65.0, 62.0 (*C*Me), 29.8, 29.7 (C*Me*) 19.7 (Me-4), 6.3 (NCH$_2$*Me*)	39.6 (1 B, FeB), 6.51 (1 B), 1.24 (1 B), −2.8 to −15.0 (m br, 6 B)
(11a)	1.31 [t of t, 12 H, *J*(HH) 7, *J*(NH) 2, NCH$_2$*Me*], 2.21 (s, 3 H, CMe), 2.47 (s, 3 H, CMe), 3.16 [q, 8 H, *J*(HH) 7, NC*H*$_2$Me], 4.02 (s, 3 H, μ_3-CMe)	304.1 [μ_3-*C*Me, *J*(WC) 107], 223.0 [WCO, *J*(WC) 150], 216.1, 215.8 (FeCO), 65.2, 59.6 (*C*Me), 44.9 (μ_3-C*Me*), 33.9, 31.8 (C*Me*), 7.7 (NCH$_2$*Me*)	[f] 55.0 [1 B, FeB(1)], 44.9 [1 B, FeB(5)], −2.2 [B(10), *J*(BH) 140], −5.8 [B(6), *J*(BH) 140], −8.6 [B(2), *J*(BH) 110], −9.5 [B(7), *J*(BH) 122], −10.7 [B(8), *J*(BH) 159], −13.5 [B(9), *J*(BH) 98], −14.4 [B(11), *J*(BH) 134]
(11b)	1.26 (m, 12 H, NCH$_2$*Me*), 2.27 (s, 3 H, CMe), 2.43 (s, 3 H, CMe), 3.09 [q, 8 H, *J*(HH) 8, NC*H*$_2$Me], 7.30—7.47 (m, 5 H, Ph)	273.0 (μ_3-*C*Ph), 222.2 [WCO, *J*(WC) 153], 210.1, 209.7 (FeCO), 156.8 [C^1 (Ph)], 129.7—125.2 (Ph), 66.8, 63.6 (*C*Me), 31.5, 31.3 (C*Me*), 7.7 (NCH$_2$*Me*)	[g] 56.1 (1 B, FeB), 46.1 (1 B, FeB), −1.7 (1 B), −5.2 (1 B), −8.8 (3 B), −13.1 (2 B)
(11c)	1.35 [t of t, 12 H, *J*(HH) 7, *J*(NH) 2, NCH$_2$*Me*], 2.26, 2.40, 2.43 (s × 3, 9 H, CMe and Me-4), 3.23 [q, 8 H, *J*(HH) 7, NC*H*$_2$Me], 7.15—7.27 (m, 4 H, C$_6$H$_4$)	271.8 (μ_3-*C*C$_6$H$_4$Me-4), 222.1, 220.6 (WCO), 213.7, 208.5, 208.1 (FeCO), 158.4 [C^1 (C$_6$H$_4$)], 133.3, 128.2, 125.4 (C$_6$H$_4$), 63.4, 58.5 (*C*Me), 32.3, 30.2 (C*Me*), 19.7 (Me-4), 6.3 (NCH$_2$*Me*)	55.9 (1 B, FeB), 45.1 (1 B, FeB), −1.5 to −15.0 (br, 7 B)
(15)	2.20 (s, 3 H, CMe), 2.36 (s, 3 H, CMe), 3.81 (s br, 3 H, μ_3-CMe), 7.40—7.47 (m, 15 H, Ph)	317.3 (μ_3-C), 220.4, 219.9 (WCO), 214.2, 213.2, 212.3, 211.5 (FeCO), 209.5 [d, *J*(PC) 5, FeCO], 206.0 [d, *J*(PC) 5, FeCO], 134.5 [d, *J* (PC) 22, C^1 (Ph)], 134.1 [d, *J*(PC) 15, C^2 and C^6 (Ph)], 132.0 [C^4 (Ph)], 129.6 [d, *J*(PC) 10, C^3 and C^5 (Ph)], 65.3, 62.1 (*C*Me), 46.1 (μ_3-C*Me*), 33.1, 32.2 (C*Me*)	52.5 (1 B, FeB), 42.9 (1 B, FeB),—1.1 to −11.7 (br, 7 B)

[a] Chemical shifts (δ) in p.p.m., coupling constants in Hz. [b] Measured in CD$_2$Cl$_2$. [c] Proton resonances of B–H groups occur as broad unresolved signals in the range δ 0—3. [d] Hydrogen-1 decoupled, chemical shifts are positive to high frequency of SiMe$_4$, with measurements in CD$_2$Cl$_2$–CH$_2$Cl$_2$ at −40 °C. Signals for N*C*H$_2$Me nuclei obscured by solvent peaks. [e] Hydrogen-1 decoupled, measured at 28 MHz, chemical shifts are positive to high frequency of BF$_3$·Et$_2$O (external), with measurements in CD$_2$Cl$_2$–CH$_2$Cl$_2$ unless otherwise stated. [f] Atom labels refer to Figure 2; assignments made from ^{11}B–^{11}B two-dimensional COSY n.m.r. spectrum, measured at 126 MHz; *J*(BH) values measured from ^{1}H-coupled spectrum. [g] Measured in (CD$_3$)$_2$CO.

Table 3. Selected internuclear distances (Å) and angles (°) for the complex [NEt$_4$][FeW{μ-CH(C$_6$H$_4$Me-4)}(μ-σ:η^5-C$_2$B$_9$H$_8$Me$_2$)(μ-CO)(CO)$_5$] **(10b)**

W–Fe	2.625(1)	W–C(4)	2.172(5)	W–C(5)	1.972(6)	W–C(6)	1.961(5)
W–C(7)	2.172(5)	W–B(5)	2.193(5)	Fe–C(1)	1.805(6)	Fe–C(2)	1.808(5)
Fe–C(3)	1.773(6)	Fe–C(4)	2.021(4)	Fe–C(7)	2.153(5)	Fe–B(5)	2.137(6)
C(1)–O(1)	1.134(8)	C(2)–O(2)	1.131(7)	C(3)–O(3)	1.158(8)	C(4)–O(4)	1.173(6)
C(5)–O(5)	1.151(8)	C(6)–O(6)	1.151(7)	C(7)–C(8)	1.478(7)	C(7)–H(71)	0.91(4)
* Mean N–C	1.512(8)	* Mean C–C	1.507(10)				
Fe–W–C(4)	48.7(1)	Fe–W–C(5)	121.3(2)	Fe–W–C(6)	117.0(2)	C(4)–W–C(5)	121.6(2)
C(4)–W–C(6)	68.8(2)	C(5)–W–C(6)	82.1(2)	Fe–W–C(7)	52.3(1)	C(4)–W–C(7)	76.3(2)
C(5)–W–C(7)	69.0(2)	C(6)–W–C(7)	111.6(2)	Fe–W–B(5)	51.7(1)	W–Fe–C(1)	128.4(2)
W–Fe–C(2)	114.9(2)	C(1)–Fe–C(2)	97.9(3)	W–Fe–C(3)	118.0(2)	C(1)–Fe–C(3)	93.5(3)
C(2)–Fe–C(3)	98.3(3)	W–Fe–C(4)	53.9(1)	C(1)–Fe–C(4)	87.7(2)	C(2)–Fe–C(4)	167.7(2)
C(3)–Fe–C(4)	92.3(2)	W–Fe–C(7)	53.0(1)	C(1)–Fe–C(7)	91.4(2)	C(2)–Fe–C(7)	89.0(2)
C(3)–Fe–C(7)	170.5(2)	C(4)–Fe–C(7)	79.9(2)	W–Fe–B(5)	53.7(1)	Fe–C(1)–O(1)	176.7(6)
Fe–C(2)–O(2)	177.4(5)	Fe–C(3)–O(3)	179.2(6)	W–C(4)–Fe	77.4(2)	W–C(4)–O(4)	149.3(3)
Fe–C(4)–O(4)	133.2(3)	W–C(5)–O(5)	179.3(6)	W–C(6)–O(6)	176.1(5)	W–C(7)–Fe	74.7(2)
W–C(7)–C(8)	131.4(3)	Fe–C(7)–C(8)	116.4(3)	W–B(5)–Fe	74.6(2)		
* Mean C–N–C	109.5(4)	* Mean N–C–C	115.7(5)				

* Tetraethylammonium cation.

ligand but evidently B(5) (Figure 1) is preferred. We have previously shown, however, that site-exchange of atoms within the pentagonal C$_2$B$_3$ ring of the ligand is facile.[4]

In the light of previous work, it is probable that the hydrogen atom, H(71), attached to C(7) of the bridging *p*-tolylmethylidene ligand was originally bonded to B(5). Thus treatment of **(6a)** with hex-3-yne results in insertion of the μ-CC$_6$H$_4$Me-4 group into the three-centre B–H $\rightharpoonup$ Mo bond to produce [MoW{μ-σ:η^5-CH(C$_6$H$_4$Me-4)C$_2$B$_9$H$_8$}(CO)$_3$(η-EtC$_2$Et)(η^5-C$_9$H$_7$)] **(14)**, containing a B–CH(C$_6$H$_4$Me-4)–Mo bridge

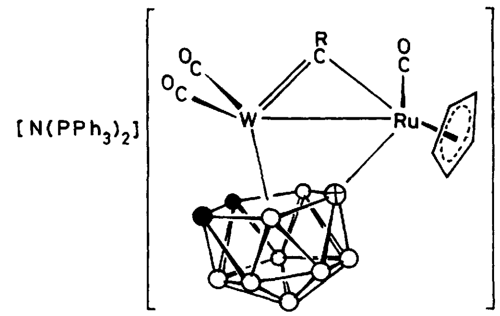

(12)

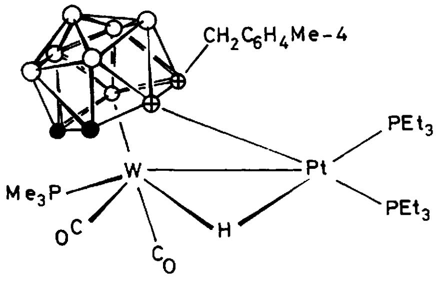

(13)

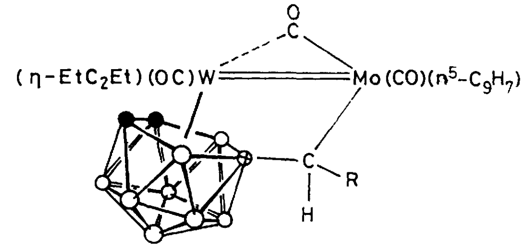

(14)

○ BH ● CMe ⊕ B

R = C$_6$H$_4$Me-4

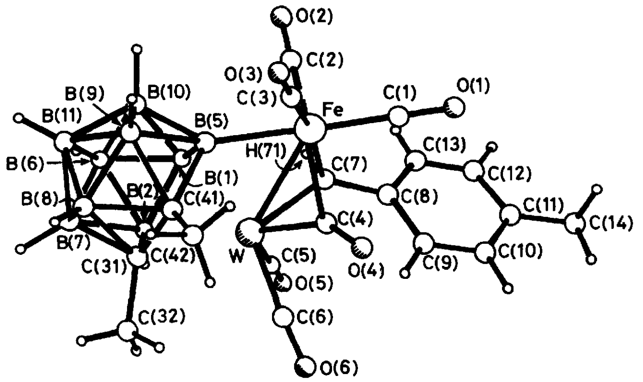

Figure 1. Structure of the anion of (**10b**), $[FeW\{\mu\text{-}CH(C_6H_4Me\text{-}4)\}(\mu\text{-}\sigma:\eta^5\text{-}C_2B_9H_8Me_2)(\mu\text{-}CO)(CO)_5]^-$, with the atom labelling scheme

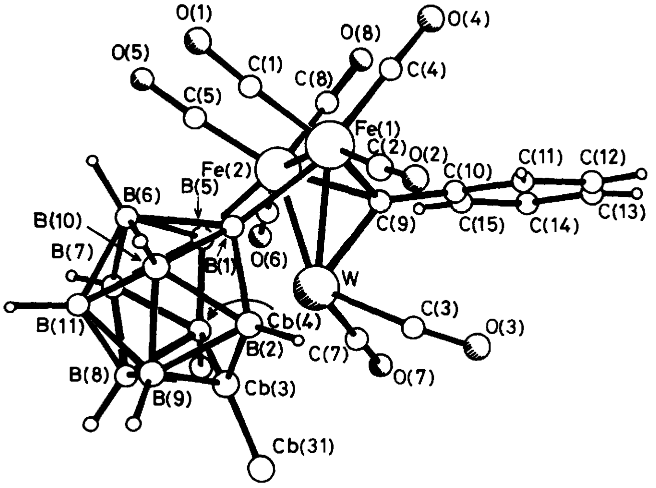

Figure 2. Structure of the anion of (**11b**), $[Fe_2W(\mu_3\text{-}CPh)(\mu\text{-}\sigma:\sigma',\eta^5\text{-}C_2B_9H_7Me_2)(CO)_8]^-$, with the atom labelling scheme

system.[8] Moreover, formation of (**7**) from (**1c**) and $[PtH(Me_2CO)(PEt_3)_2][BF_4]$ involves addition of B–H, and hydride derived from the platinum reagent, to the CC_6H_4Me-4 fragment.[5]

The structure of the anion of (**11b**) is shown in Figure 2, and is without precedent in the field of carbametallaborane chemistry. Selected structural parameters are given in Table 4. On one side of the isosceles triangle of metal atoms [Fe–Fe 2.578(2), Fe–W (mean) 2.645(2) Å] the carbaborane ligand adopts a 'slipped' η^5-bonding mode to the tungsten, and is linked to the iron atoms by σ bonds [Fe(1)–B(1) 2.12(1), Fe(2)–B(5) 2.14(1) Å]. Formally the ligand contributes six electrons to the trimetal anion which is overall a 48-valence-electron species. The B(1)–B(5) connectivity lies parallel to the Fe(1)–Fe(2) bond. An approximate non-crystallographic mirror plane bisects the anion, passing through the tungsten perpendicular to the Fe_2W triangle and bisecting the Fe(1)–Fe(2) vector. There is an atom site disorder, refined to 72%, between the B(2) and Cb(4) positions. The major occupant has B(2) adjacent to B(1) and Cb(4)–Cb(41) adjacent to B(5). The slip distance (Δ)[7] of the tungsten towards the mid-point of B(1)–B(5) is 0.19 Å, while the fold angles θ and φ between the perpendicular through the centroid of B(6)B(7)B(8)B(9)B(10) and the planes defined by B(2)B(1)B(5)Cb(4) and by B(2)Cb(3)Cb(4) are 0.7 and 2.1°, respectively.

Each iron atom is ligated by three terminally bound carbonyl groups, and the tungsten atom by two such groups. A phenylmethylidyne group triply bridges the Fe_2W triangle on the opposite side to the carbaborane ligand but is significantly closer to the tungsten atom [W–C(9) 2.029(8), Fe(1)–C(9) 2.066(8), Fe(2)–C(9) 2.06(1) Å].

Having established the structures of (**10b**) and (**11b**), and by

Table 4. Selected internuclear distances (Å) and angles (°) for the complex $[NEt_4][Fe_2W(\mu_3\text{-}CPh)(\mu\text{-}\sigma:\sigma',\eta^5\text{-}C_2B_9H_7Me_2)(CO)_8]$ (**11b**)

W–Fe(1)	2.647(2)	W–Fe(2)	2.644(2)	W–C(3)	2.03(1)	W–C(7)	1.991(9)
W–C(9)	2.029(8)	W–B(1)	2.17(1)	W–B(5)	2.18(1)	Fe(1)–Fe(2)	2.578(2)
Fe(1)–C(1)	1.74(1)	Fe(1)–C(2)	1.78(2)	Fe(1)–C(4)	1.77(1)	Fe(1)–C(9)	2.066(8)
Fe(1)–B(1)	2.12(1)	Fe(2)–C(5)	1.76(1)	Fe(2)–C(6)	1.79(1)	Fe(2)–C(8)	1.77(1)
Fe(2)–C(9)	2.06(1)	Fe(2)–B(5)	2.14(1)	C(1)–O(1)	1.17(1)	C(2)–O(2)	1.15(2)
C(3)–O(3)	1.15(2)	C(4)–O(4)	1.15(1)	C(5)–O(5)	1.17(1)	C(6)–O(6)	1.14(1)
C(7)–O(7)	1.17(1)	C(8)–O(8)	1.16(1)	C(9)–C(10)	1.49(1)		
* Mean N–C	1.50(2)	* Mean C–C	1.55(2)				

Fe(1)–W–Fe(2)	58.3(1)	W–Fe(1)–Fe(2)	60.8(1)	W–Fe(2)–Fe(1)	60.9(1)	Fe(1)–W–C(3)	92.6(2)
Fe(2)–W–C(3)	135.2(3)	Fe(1)–W–C(7)	135.8(3)	Fe(2)–W–C(7)	94.8(3)	C(3)–W–C(7)	83.5(4)
Fe(1)–W–C(9)	50.4(2)	Fe(2)–W–C(9)	50.2(3)	C(3)–W–C(9)	85.1(4)	C(7)–W–C(9)	85.4(3)
W–Fe(1)–C(1)	125.4(3)	Fe(2)–Fe(1)–C(1)	98.2(4)	W–Fe(1)–C(2)	97.6(3)	Fe(2)–Fe(1)–C(2)	157.6(3)
C(1)–Fe(1)–C(2)	99.4(5)	W–Fe(1)–C(4)	133.4(3)	Fe(2)–Fe(1)–C(4)	95.9(4)	C(1)–Fe(1)–C(4)	95.7(5)
C(2)–Fe(1)–C(4)	95.9(5)	W–Fe(1)–C(9)	49.1(2)	Fe(2)–Fe(1)–C(9)	51.2(3)	W–Fe(2)–C(5)	126.4(4)
Fe(1)–Fe(2)–C(5)	97.8(4)	W–Fe(2)–C(6)	99.2(4)	Fe(1)–Fe(2)–C(6)	158.3(4)	C(5)–Fe(2)–C(6)	101.5(5)
W–Fe(2)–C(8)	133.3(4)	Fe(1)–Fe(2)–C(8)	94.9(4)	C(5)–Fe(2)–C(8)	93.9(5)	C(6)–Fe(2)–C(8)	93.6(5)
W–Fe(2)–C(9)	49.2(2)	Fe(1)–Fe(2)–C(9)	51.5(2)	C(5)–Fe(2)–C(9)	148.6(4)	C(6)–Fe(2)–C(9)	109.9(5)
C(8)–Fe(2)–C(9)	84.2(5)	Fe(1)–C(1)–O(1)	175.0(9)	Fe(1)–C(2)–O(2)	176(1)	W–C(3)–O(3)	176.9(7)
Fe(1)–C(4)–O(4)	179.4(9)	Fe(2)–C(5)–O(5)	176.0(9)	Fe(2)–C(6)–O(6)	177.4(9)	W–C(7)–O(7)	177.7(8)
Fe(2)–C(8)–O(8)	179(1)	Mean W–C(9)–Fe	80.6(4)	Fe(1)–C(9)–Fe(2)	77.4(3)	W–C(9)–C(10)	137.0(6)
Mean Fe–C(9)–C(10)	129.8(7)	W–B(1)–Fe(1)	76.1(4)	W–B(5)–Fe(2)	75.6(4)	* Mean C–N–C	109.5(8)
* Mean N–C–C	113(1)						

* Tetraethylammonium cation.

inference those of (**10a**), (**11a**), and (**11c**) also, it is possible to interpret the i.r. and n.m.r. data for these species. The dimetal compounds show six bands in the carbonyl stretching region of their i.r. spectra, and one of these absorptions [1 754 for (**10a**), 1 755 cm^{-1} for (**10b**)] corresponds to a bridging mode. In the ^1H n.m.r. spectra (Table 2) resonances at δ 6.67 for (**10a**) and 6.39 for (**10b**) may be assigned to the μ-CH groups. The corresponding signal in the ^1H n.m.r. spectrum of $[PtW(\mu\text{-}H)\{\mu\text{-}CH(C_6H_4Me\text{-}4)\}(CO)_2(PMe_3)_2(\eta\text{-}C_5H_5)]$ occurs at δ 6.57 and in several complexes with $\mu\text{-}C\mathit{H}(C_6H_4Me\text{-}4)$ groups we have observed peaks for the alkylidene hydrogen in the range δ 4.66—6.71.[9]

In the $^{13}C\text{-}\{^1H\}$ n.m.r. spectra of (**10a**) and (**10b**) there are characteristic resonances for the μ-C nuclei [δ 119.8 for (**10a**), 119.3 p.p.m. for (**10b**)]. In the spectrum of the complex $[PtW(\mu\text{-}H)\{\mu\text{-}CH(C_6H_4Me\text{-}4)\}(CO)_2(PMe_3)_2(\eta\text{-}C_5H_5)]$, mentioned above, the μ-C signal is at δ 105.3 p.p.m.[9] The CO groups in the complexes (**10**) give rise to two signals of equal intensity, the peaks corresponding to FeCO and WCO groups (Table 2). These may be assigned on the basis of their chemical shifts, and by the observations of $^{183}W\text{-}^{13}C$ coupling on the peak at δ 233.7 p.p.m. in the spectrum of (**10a**). The overall pattern of two peaks indicates that site-exchange processes occur between the two CO ligands terminally bound to tungsten and the bridging CO group and between the CO groups terminally bound to the iron even at −40 °C, the temperature of the measurement. The $^{13}C\text{-}\{^1H\}$ n.m.r. spectra of (**10**) also show diagnostic signals for the CMe groups of the carbaborane ligand. Moreover, the shifts for the *C*Me nuclei [δ 63.6 and 66.8 for (**10a**), 62.0 and 65.0 p.p.m. for (**10b**)] are in the expected region for such groups.

The $^{11}B\text{-}\{^1H\}$ n.m.r. spectra of the complexes (**10**) clearly reveal the presence of the B–Fe σ bonds with characteristic resonances at δ 40.7 for (**10a**) and 39.6 p.p.m. for (**10b**). In compounds (**12**)[3] and (**13**)[5] the B–Ru and B–Pt groups give rise to signals in their $^{11}B\text{-}\{^1H\}$ spectra at δ 45.9 and 36.2 p.p.m., respectively. The remaining boron nuclei in (**10a**) and (**10b**) give rise to broad $^{11}B\text{-}\{^1H\}$ n.m.r. resonances to higher field (*ca.* 6.5 to −15.0 p.p.m.).

The n.m.r. spectra of the trimetal compounds (**11**), data for which are summarised in Table 2, also accord with the structure established for (**11b**) by *X*-ray diffraction. The $^{13}C\text{-}\{^1H\}$ n.m.r. spectra show characteristic resonances for the μ_3-C nuclei [δ 304.1, 273.0, and 271.8 p.p.m. for (**11a**), (**11b**), and (**11c**) respectively]. A $^{11}B\text{-}^{11}B$ two-dimensional COSY n.m.r. spectrum of (**11a**) allowed the observation of nine resonances which could be assigned as indicated in Table 2. Peaks at δ 44.9 and 55.0 p.p.m. are due to the two B–Fe σ bonds, cross peaks between which agree with the presence of a B–B bond. Peaks in the $^{11}B\text{-}\{^1H\}$ spectra of (**11b**) at δ 46.1 and 56.1 p.p.m., and of (**11c**) at δ 45.1 and 55.9 p.p.m. may be attributed to the B–Fe groups in these species.

The mechanisms by which the compounds (**10**) and (**11**) are formed are not known at the present time, but there is evidence that the species (**9**) are intermediates. We have recently prepared a stable dimetal compound of type (**9**) having a bridging $CC_6H_3Me_2\text{-}2,6$ group. The presence of methyl groups as *ortho* substituents in the aromatic ring appears to inhibit rearrangement or further reaction with carbonyl–iron fragments. Moreover, during the syntheses of mixtures of (**10a**) and (**11b**), from (**1b**) and $[Fe_3(CO)_{12}]$, we have observed a transient species which shows a $^{13}C\text{-}\{^1H\}$ n.m.r. resonance for a μ-C group at δ 381.3 p.p.m. This intermediate may be the complex (**9**, R = Ph), on the basis of the relatively deshielded chemical shift observed for the μ-C nucleus.[6] Formation of the saturated 34-valence-electron compounds (**10a**) and (**10b**) from the unsaturated 32-valence-electron dimetal precursors (**9**, R = Ph or $C_6H_4Me\text{-}4$) might proceed *via* the intermediacy of a species with a B–H ⇀ Fe three-centre two-electron bond employing a boron atom in the pentagonal face of the carborane ligand. In a subsequent step hydrogen transfer to the alkylidyne ligand and CO capture might occur with concomitant formation of the B–Fe σ bond. However, (**10a**) and (**10b**) are the minor products of the reactions which afford (**11b**) and (**11c**), respectively. Moreover, as mentioned earlier, an iron–tungsten dimetal compound was not obtained from (**1a**) and $[Fe_2(CO)_9]$. It would thus appear from these results that the species (**9**), if formed initially react with a carbonyl–iron fragment more rapidly than they add CO and isomerise to (**10**). Addition of an

Table 5. Atomic positional parameters (fractional co-ordinates × 10^4) for complex (**10b**), with estimated standard deviations in parentheses

Atom	*x*	*y*	*z*	Atom	*x*	*y*	*z*
W	4 821(1)	1 399(1)	2 148(1)	B(1)	4 202(4)	−2(3)	1 457(3)
Fe	3 684(1)	2 085(1)	657(1)	B(2)	4 702(4)	−158(4)	2 586(4)
C(1)	3 878(4)	3 073(4)	103(3)	C(31)	4 153(4)	547(3)	3 036(3)
O(1)	3 960(4)	3 710(3)	−246(4)	C(41)	3 384(4)	1 212(3)	2 347(3)
C(2)	3 334(4)	1 296(4)	−240(3)	B(5)	3 388(4)	932(4)	1 295(3)
O(2)	3 102(3)	830(3)	−823(2)	B(6)	3 781(5)	−897(4)	1 897(4)
C(3)	2 523(4)	2 444(4)	548(3)	B(7)	3 763(5)	−571(4)	2 890(5)
O(3)	1 764(3)	2 683(4)	467(3)	B(8)	2 927(5)	298(5)	2 719(5)
C(4)	4 316(3)	2 784(3)	1 775(3)	B(9)	2 456(4)	569(4)	1 623(4)
O(4)	4 279(3)	3 547(2)	1 969(2)	B(10)	2 943(4)	−201(4)	1 096(4)
C(5)	6 148(4)	1 036(4)	2 360(4)	B(11)	2 684(5)	−570(5)	1 969(5)
O(5)	6 921(3)	826(4)	2 475(3)	C(32)	4 613(5)	841(5)	3 993(3)
C(6)	5 481(4)	2 267(4)	3 080(3)	C(42)	3 051(4)	2 088(4)	2 635(4)
O(6)	5 845(4)	2 815(3)	3 595(3)	N	9 437(3)	1 325(3)	1 956(3)
C(7)	5 148(3)	1 652(3)	1 016(3)	C(15)	8 975(4)	535(5)	1 378(4)
C(8)	5 802(3)	2 313(3)	861(3)	C(16)	9 650(5)	−30(4)	1 110(4)
C(9)	6 185(4)	3 083(4)	1 368(3)	C(17)	10 170(4)	1 012(5)	2 802(3)
C(10)	6 738(4)	3 717(3)	1 150(4)	C(18)	9 782(7)	419(5)	3 338(5)
C(11)	6 968(4)	3 597(3)	432(4)	C(19)	8 633(4)	1 862(5)	2 107(4)
C(12)	6 634(4)	2 810(4)	−51(3)	C(20)	8 941(5)	2 625(4)	2 748(5)
C(13)	6 075(3)	2 186(3)	161(3)	C(21)	9 955(4)	1 943(4)	1 561(4)
C(14)	7 547(4)	4 299(4)	185(4)	C(22)	9 379(6)	2 289(6)	665(5)

Table 6. Atomic positional parameters (fractional co-ordinates × 10^4) for complex (**11b**), with estimated standard deviations in parentheses

Atom	*x*	*y*	*z*	Atom	*x*	*y*	*z*
W	5 300(1)	2 143(1)	2 117(1)	Hb(2a)	6 279	3 788	1 282
Fe(1)	3 471(1)	2 183(1)	1 018(1)	Hb(2b)	6 088	4 453	1 815
Fe(2)	3 601(1)	1 395(1)	2 131(1)	Hb(2c)	5 668	4 875	1 067
C(1)	2 488(7)	3 118(8)	855(5)	Cb(3)	6 240(7)	3 717(8)	2 715(4)
O(1)	1 801(5)	3 722(6)	697(4)	Cb(31)	7 414(7)	3 588(10)	2 991(5)
C(2)	3 911(8)	2 652(9)	436(6)	Hb(3a)	7 585	3 771	2 633
O(2)	4 142(7)	2 998(8)	46(4)	Hb(3b)	7 708	2 901	3 177
C(3)	6 068(7)	1 827(8)	1 568(5)	Hb(3c)	7 692	4 124	3 342
O(3)	6 465(6)	1 622(7)	1 238(4)	B(4)	5 558(7)	3 096(8)	3 066(5)
C(4)	2 642(8)	1 170(8)	478(5)	Cb(4)	5 558(7)	3 096(8)	3 066(5)
O(4)	2 096(6)	517(6)	126(4)	Cb(41)	6 148(12)	2 498(13)	3 743(7)
C(5)	2 610(7)	2 162(9)	2 166(5)	Hb(4a)	5 875	1 870	3 856
O(5)	1 912(5)	2 619(6)	2 174(4)	Hb(4b)	6 069	3 107	3 980
C(6)	4 181(8)	776(9)	2 952(5)	Hb(4c)	6 872	2 391	3 873
O(6)	4 517(6)	357(7)	3 467(4)	B(5)	4 294(9)	2 939(10)	2 468(6)
C(7)	6 229(7)	1 010(8)	2 731(5)	B(6)	3 776(9)	4 252(11)	2 221(6)
O(7)	6 747(6)	320(6)	3 087(4)	B(7)	4 658(9)	3 970(11)	3 092(6)
C(8)	2 777(8)	287(9)	1 733(5)	B(8)	5 872(10)	4 462(11)	3 217(6)
O(8)	2 242(6)	−433(7)	1 461(4)	B(9)	5 778(10)	5 000(11)	2 472(6)
C(9)	4 360(7)	908(7)	1 588(4)	B(10)	4 490(9)	4 855(11)	1 821(6)
C(11)	4 536(4)	−333(4)	764(3)	B(11)	4 762(10)	5 156(11)	2 678(6)
C(12)	4 776	−1 340	598	N	8 473(5)	2 942(6)	246(3)
C(13)	4 968	−2 205	1 041	C(21)	8 169(9)	2 299(10)	695(5)
C(14)	4 920	−2 061	1 651	C(22)	8 728(10)	2 681(11)	1 442(5)
C(15)	4 680	−1 054	1 818	C(31)	9 591(10)	2 778(10)	440(7)
C(10)	4 488	−190	1 374	C(32)	9 862(11)	1 596(11)	375(7)
B(1)	4 194(8)	3 455(10)	1 718(5)	C(41)	8 344(9)	4 119(11)	320(6)
B(2)	5 443(8)	3 948(9)	1 874(5)	C(42)	7 231(9)	4 387(11)	208(7)
Cb(2)	5 443(8)	3 948(9)	1 874(5)	C(51)	7 770(8)	2 541(9)	−466(5)
Cb(21)	5 798(22)	4 245(27)	1 346(13)	C(52)	7 986(10)	3 077(10)	−1 015(6)

$Fe(CO)_4$ group to (**9**) could give trimetal complexes $[NEt_4][Fe_2W(\mu_3\text{-}CR)(\eta^5\text{-}C_2B_9H_9Me_2)(\mu\text{-}CO)(CO)_8]$. The $\eta^5\text{-}C_2B_9H_9Me_2$ ligand in the latter might then form two B–Fe bonds to yield the product (**11**). Such a process would necessitate loss of hydrogen from the two BH groups and also a molecule of CO. The hydrogen might well be transferred to carbonyl–iron groups, thus accounting for the appreciable amounts of $[NEt_4][Fe_3(\mu\text{-}H)(CO)_{11}]$ observed as a by-product in the reactions.

Attempts to isolate neutral complexes from the compounds (**10**) and (**11**) by protonation have so far been unsuccessful. However, in view of the isolobal relationship between the groups H^+ and $[Au(PPh_3)]^+$ the reaction between (**11a**) and $[AuCl(PPh_3)]$ in thf in the presence of $TlPF_6$ was studied. The thallium salt was added to facilitate removal of chloride as insoluble TlCl, generating $[Au(PPh_3)]^+$ *in situ*. The product was a tetranuclear metal complex formulated as $[AuFe_2W(\mu_3\text{-}CMe)(\mu\text{-}\sigma{:}\sigma',\eta^5\text{-}C_2B_9H_7Me_2)(CO)_8(PPh_3)]$ (**15**), data for which are

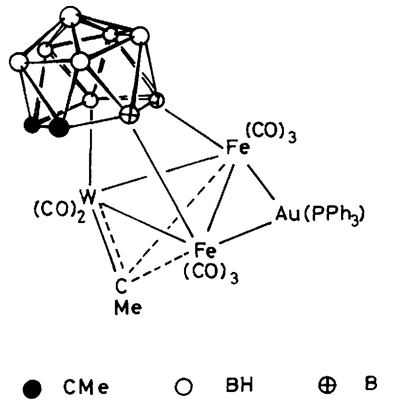

(15)

given in Tables 1 and 2. Compound (15) is soluble in CH_2Cl_2, toluene, Et_2O, and thf. However, solutions in CH_2Cl_2 decompose after a few hours, and in thf i.r. bands due to the anion $[Fe_2W(\mu_3\text{-}CMe)(\mu\text{-}\sigma{:}\sigma',\eta^5\text{-}C_2B_9H_7Me_2)(CO)_8]^-$ appear on standing. Chlorobenzene solutions of (15) on treatment with NEt_4Cl regenerate the salt (11a) quantitatively. The $Au(PPh_3)$ fragment is presumably lost in this reaction as $[AuCl(PPh_3)]$.

Examination of the n.m.r. spectra of (15) (Table 2) reveal that the structure of the tetranuclear metal compound cannot be very different from that of the anion in its precursor (11a), apart from addition of the $Au(PPh_3)$ fragment. Thus the $^{11}B\text{-}\{^1H\}$ n.m.r. spectrum showed resonances at δ 42.9 and 52.5 p.p.m. characteristic for the two boron nuclei σ bonded to the iron atoms. The ^1H n.m.r. spectrum showed signals for the carbaborane CMe groups and the μ_3-CMe ligand similar to those in the spectrum of (11a). Interest centres on the location of the $Au(PPh_3)$ group. However, measurement of the $^{13}C\text{-}\{^1H\}$ n.m.r. spectrum of (15) at room temperature and at -40 °C revealed the existence of two isomers in equilibrium at ambient temperatures, but at the low-temperature limit essentially only one species is present. Thus at -40 °C, eight CO resonances are observed and on the basis of the chemical shifts two of the signals (δ 220.4 and 219.9 p.p.m.) are assigned to groups bonded to the tungsten, and six (δ 214.2, 213.2, 212.3, 211.5, 209.5, and 206.0 p.p.m.) to groups bonded to the iron atoms. Moreover, the resonances at δ 209.5 and 206.0 p.p.m. both appear as doublets [J(PC) 5 Hz], suggesting that these signals are due to FeCO groups *transoid* to the $Au(PPh_3)$ fragment which can reasonably be assumed to be bridging the Fe–Fe bond. A resonance at δ 317.3 p.p.m. is attributable to the methylidyne carbon nucleus but it is more deshielded than the corresponding signal in the spectrum of (11a) (δ 304.1 p.p.m.). This may indicate that the methylidyne ligand in (15) asymmetrically bridges the Fe_2W triangle. Generally alkylidyne carbon nuclei triply bridging a metal triangle in a symmetrical manner give rise to resonances in the range *ca.* 250—290 p.p.m., whereas if the alkylidyne ligand asymmetrically bridges a metal triangle the resonances for the μ_3-C groups occur in the range *ca.* 300—325 p.p.m.[10] When the $^{13}C\text{-}\{^1H\}$ n.m.r. spectrum of compound (15) is measured at room temperature the two WCO resonances remain sharp, but eight broad rather than six sharp FeCO signals are observed. Moreover, a resonance occurs at δ 290.2 p.p.m., in addition to that seen at δ 317.3 p.p.m. The appearance of the peak at 290.2 p.p.m. suggests the presence of an isomer of (15) with a symmetrically bridging μ_3-CMe group; the intensity of this signal is only half that at 317.3 p.p.m.

As mentioned above, the *X*-ray diffraction study of (11b) revealed the μ_3-CPh ligand to be closer to the tungsten than to the iron atoms, in spite of the radius of the former being larger than the latter. Assuming the same asymmetry for the bridging μ_3-CMe group in the anion of (11a), the observed $^{13}C\text{-}\{^1H\}$ n.m.r. signal at 304.1 p.p.m. is in accord with the expected trend, with that at δ 317.3 p.p.m. in the low-temperature spectrum of (15) indicating an even higher degree of asymmetry in the μ_3-CMe bridging mode. In the minor isomer of (15), with an alkylidyne carbon n.m.r. signal (290.2 p.p.m.) in the range for a symmetrically bridging ligand, it is possible that the $Au(PPh_3)$ fragment is σ bonded to one iron centre, rather than bridging the Fe–Fe bond. This might account for the ready displacement of the gold–phosphine group by chloride ion, mentioned above.

The results described in this paper, together with those reported earlier,[1] show that the C≡W bonds present in the salts (1) will combine with neutral metal–ligand fragments to afford di- or tri-metal anionic complexes. Moreover, the structures established for the compounds (10) and (11) provide further interesting examples of the involvement of the η^5-carbaborane ligand in these reactions. Finally, isolation of the gold-containing cluster compound (15) suggests that the complexes (11) might be useful precursors to other tetranuclear metal species.

Experimental

The techniques and equipment used have been described in earlier papers in this series.[1—5] Light petroleum refers to that fraction of b.p. 40—60 °C. The compounds $[NEt_4][W(\equiv CR)(CO)_2(\eta^5\text{-}C_2B_9H_9Me_2)]$ [R = Me (1a), Ph (1b), or C_6H_4Me-4 (1c)] were prepared as described elsewhere.[1,2]

Reactions Between the Salts $[NEt_4][W(\equiv CR)(CO)_2(\eta^5\text{-}C_2B_9H_9Me_2)]$ *and* $[Fe_2(CO)_9]$.—(*i*) Compound (1a) (1.4 g, 2.5 mmol), $[Fe_2(CO)_9]$ (3.6 g, 10 mmol), and thf (30 cm^3) were placed in a Schlenk tube under nitrogen. The $[Fe_2(CO)_9]$ dissolved in *ca.* 1 h and a black solution formed. The mixture was stirred for *ca.* 15 h at room temperature. Volatile material was removed *in vacuo*. The residue was redissolved in CH_2Cl_2 (20 cm^3) and chromatographed on an alumina column (*ca.* 3 × 12 cm), eluting with the same solvent. A fast-moving green band contained a trace of $[Fe_3(CO)_{12}]$, identified by its i.r. spectrum; the second eluate was olive coloured, and this contained the desired product. A third pink band moved only very slowly requiring *ca.* 600 cm^3 of CH_2Cl_2 for complete elution; removal of solvent *in vacuo* and measurement of the i.r. spectrum showed it to be $[NEt_4][Fe_3(\mu\text{-}H)(CO)_{11}]$ (0.33 g) by comparison with an authentic sample. The olive coloured eluate, after removal of solvent *in vacuo* afforded a dark brown residue which was dissolved in *ca.* 5—10 cm^3 of thf in a narrow Schlenk tube. If the i.r. spectrum of this solution shows the presence of $[NEt_4][Fe_3(\mu\text{-}H)(CO)_{11}]$ it must be re-chromatographed as described above. A layer of Et_2O (*ca.* 30 cm^3) was placed above the thf solution, and the Schlenk tube placed in a freezer (*ca.* -25 °C) without mixing the solvents. Within a few days black *crystals* of $[NEt_4][Fe_2W(\mu_3\text{-}CMe)(\mu\text{-}\sigma{:}\sigma',\eta^5\text{-}C_2B_9H_7Me_2)(CO)_8]$ (11a) formed and were collected (0.65 g, 31%) on a glass frit and washed with Et_2O (2 × 20 cm^3).

(*ii*) In a similar reaction, (1b) (1.5 g, 2.4 mmol) and $[Fe_2(CO)_9]$ (3.8 g, 10.4 mmol) in thf (20 cm^3) were stirred at room temperature for 24 h. Volatile material was removed *in vacuo*, and the black residue washed with light petroleum (2 × 20 cm^3) to remove $[Fe_3(CO)_{12}]$. The black residue was redissolved in CH_2Cl_2 (20 cm^3) and chromatographed on an alumina column. Eluting with the same solvent, a fast-moving green band contained more $[Fe_3(CO)_{12}]$. A brown band was next recovered, and this eluate was reduced in volume to *ca.* 5 cm^3, placed in a narrow Schlenk tube, and Et_2O (40 cm^3) layered on top. This mixture was cooled to *ca.* -25 °C and after a few days a conglomerate mixture of black *crystals* and red *microcrystals* formed (*ca.* 9:1). These were collected by filtration, washed with Et_2O ($10\ cm^3$), and dried *in vacuo* (1.16 g). The red crystals of the minor product $[NEt_4][FeW\{\mu\text{-}CH(Ph)\}(\mu\text{-}\sigma:\eta^5\text{-}C_2B_9H_8Me_2)(\mu\text{-}CO)(CO)_5]$ (**10a**) can be separated by hand picking from the major product $[NEt_4][Fe_2W(\mu_3\text{-}CPh)(\mu\text{-}\sigma:\sigma',\eta^5\text{-}C_2B_9H_7Me_2)(CO)_8]$ (**11b**). The third eluate from the chromatography column contained $[NEt_4][Fe_3(\mu\text{-}H)(CO)_{11}]$ (identified by i.r.).

A mixture (0.63 g), of compounds (**10a**) (*ca.* 8%) and (**11b**) (*ca.* 92%) was also obtained by treating (**1b**) (0.93 g, 2.5 mmol) portionwise with $[Fe_3(CO)_{12}]$ (0.79 g, 1.5 mmol) in thf ($20\ cm^3$). Work-up of this reaction mixture was effected as described earlier.

(*iii*) Compound (**1c**) (2.3 g, 3.6 mmol) was dissolved in thf ($30\ cm^3$) and treated with $[Fe_2(CO)_9]$ (5.7 g, 15.6 mmol). The mixture was stirred (24 h), and then all volatile material was removed *in vacuo*. The residue was dissolved in CH_2Cl_2 ($20\ cm^3$) and chromatographed on alumina, eluting with the same solvent. The first green eluate contained $[Fe_3(CO)_{12}]$ (*ca.* 20 mg), identified by i.r. The second eluate was brown in colour and this was followed by a pink eluate containing $[NEt_4][Fe_3(\mu\text{-}H)(CO)_{11}]$ (*ca.* 0.412 g). The dark brown eluate was reduced in volume to *ca.* 5—10 cm^3, and a layer of Et_2O ($50\ cm^3$) was added. This mixture was cooled to *ca.* −25 °C. After a few days black and dark brown *microcrystals* (1.31 g, *ca.* 40%) formed, and the i.r. spectrum revealed these crystals to be a *ca.* 1:9 mixture of (**10b**) and (**11c**). The crude mixture (0.87 g) was redissolved in thf ($5\ cm^3$) which was again layered with Et_2O ($30\ cm^3$) and cooled to −25 °C for 2 d. This afforded a mixture (0.64 g) of dark red *crystals* of $[NEt_4][FeW\{\mu\text{-}CH(C_6H_4Me\text{-}4)\}(\mu\text{-}\sigma:\eta^5\text{-}C_2B_9H_8Me_2)(\mu\text{-}CO)(CO)_5]$ (**10b**) and black *microcrystals* of $[NEt_4][Fe_2W(\mu_3\text{-}CC_6H_4Me\text{-}4)(\mu\text{-}\sigma:\sigma',\eta^5\text{-}C_2B_9H_7Me_2)(CO)_8]$ (**11c**). The crystals were separated by hand and those of (**10b**) used for the *X*-ray diffraction study.

Reaction Between the Salt $[NEt_4][Fe_2W(\mu_3\text{-}CMe)(\mu\text{-}\sigma:\sigma',\eta^5\text{-}C_2B_9H_7Me_2)(CO)_8]$ *and* $[AuCl(PPh_3)]$.—Solid $[AuCl(PPh_3)]$ (0.62 g, 1.25 mmol) was added portionwise to a stirred mixture of (**11a**) (0.21 g, 0.25 mmol) and $TlPF_6$ (0.60 g, 1.70 mmol) in thf ($12\ cm^3$). The progress of the reaction was monitored by i.r., but total conversion occurs only if a large excess of the gold complex is used. Solvent was removed *in vacuo*, and the residue extracted with Et_2O ($3 \times 10\ cm^3$). The extracts were filtered through a Celite pad (0.5 × 3 cm) and concentrated to *ca.* 10 cm^3. Light petroleum ($10\ cm^3$) was added, and the solution cooled to *ca.* −20 °C for 15 h to afford, after filtration and washing the solid with light petroleum ($10\ cm^3$), black *microcrystals* of $[AuFe_2W(\mu_3\text{-}CMe)(\mu\text{-}\sigma:\sigma',\eta^5\text{-}C_2B_9H_7Me_2)(CO)_8(PPh_3)]$ (**15**) (0.16 g, 54%).

Crystal Structure Determinations.—Crystals of the dimetal compound (**10b**) grow as large red rhombs, those of the trimetal compound (**11b**) as small black cuboids. Crystals for study [(**10b**), *ca.* 0.5 × 0.5 × 0.6 mm; (**11b**), 0.25 × 0.30 × 0.15 mm] were sealed in Lindemann glass capillaries under dry nitrogen. Diffracted intensities were collected (ω–2θ scans) in the range $2.9 \leqslant 2\theta \leqslant 50°$ at 298 K for (**10b**) and $2.9 \leqslant 2\theta \leqslant 40°$ for (**11b**) on a Nicolet *P*3*m* four-circle diffractometer. For (**10b**), of 6 783 intensities, 4 815 had $I \geqslant 3\sigma(I)$, where $\sigma(I)$ is the standard deviation in I based on counting statistics. Only these data were used in final refinement of the structure, after all the data had been corrected for Lorentz and polarisation effects, and an empirical correction applied for *X*-ray absorption.[11] Correspondingly for (**11b**), of 3 833 intensities, 2 589 had $I \geqslant 3\sigma(I)$ and only these were used in refinement, after similar corrections had been applied.

Crystal data for (**10b**). $[C_8H_{20}N]^+[C_{18}H_{22}B_9FeO_6W]^-$, $M = 801.6$, monoclinic, $a = 15.133(4)$, $b = 14.649(5)$, $c = 16.779(5)$ Å, $\beta = 112.82(2)°$, $U = 3\,429(2)$ Å^3, $D_c = 1.55$ g cm^{-3}, $Z = 4$, $F(000) = 1\,592$, space group $P2_1/n$ (non-standard, no. 14), Mo-K_α *X*-radiation (graphite monochromator), $\bar{\lambda} = 0.710\,69$ Å, μ(Mo-K_α) = 38.85 cm^{-1}.

Crystal data for (**11b**). $[C_8H_{20}N]^+[C_{19}H_{18}B_9Fe_2O_8W]^-$, $M = 897.5$, monoclinic, $a = 14.490(6)$, $b = 12.445(5)$, $c = 22.141(5)$ Å, $\beta = 117.42(2)°$, $U = 3\,544(2)$ Å^3, $D_c = 1.68$ g cm^{-3}, $Z = 4$, $F(000) = 1\,768$, space group $P2_1/n$ (non-standard, no. 14), μ(Mo-K_α) = 41.62 cm^{-1}.

Structure solutions and refinements. The structures were solved by heavy-atom methods, and all non-hydrogen atoms were located from difference-Fourier calculations. All refinements, by blocked-cascade least-squares techniques, were performed on a Data General 'Eclipse' computer with the SHELXTL system of programs.[11] For (**10b**), the hydrogen atoms attached to the boron atoms of the carbaborane cage, the four aromatic hydrogens of the *p*-tolyl group, and H(71) were located from difference-Fourier calculations. All the tetraethylammonium cation hydrogens and the remaining methyl group hydrogens in(**10b**), and, due to the paucity of the data for (**11b**), all the hydrogen atoms of the latter, were incorporated at calculated positions (C–H 0.96, B–H 1.10 Å) with tied isotropic thermal parameters (1.2 times $U_{eq.}$ for the atom to which they were attached). Weighting schemes applied were of the form $w = [\sigma^2(F_o) + g|F_o|^2]^{-1}$ where $g = 0.0002$ for (**10b**) and (**11b**). The final difference density synthesis showed no peaks > 1 e Å^{-3} for either structure. Scattering factors for W were taken from ref. 12, while those for all other atoms are included in the programs of ref. 11. Refinement converged at $R = 0.029$ ($R' = 0.030$) for (**10b**), and $R = 0.034$ ($R' = 0.034$) for (**11b**). Atomic co-ordinates are listed in Tables 5 and 6.

Acknowledgements

We thank the Deutscher Akademischer Austauschdienst for the award of a N.A.T.O. Fellowship (to F-E. B.) and the U.S.A.F. Office of Scientific Research (Grant 86-0125) for partial support.

References

1 Part 67, F.-E. Baumann, J. A. K. Howard, O. Johnson, and F. G. A. Stone, *J. Chem. Soc., Dalton Trans.*, 1987, 2661.
2 M. Green, J. A. K. Howard, A. P. James, C. M. Nunn, and F. G. A. Stone, *J. Chem. Soc., Dalton Trans.*, 1987, 61.
3 M. Green, J. A. K. Howard, A. N. de M. Jelfs, O. Johnson, and F. G. A. Stone, *J. Chem. Soc., Dalton Trans.*, 1987, 73.
4 M. Green, J. A. K. Howard, A. P. James, A. N. de M. Jelfs, C. M. Nunn, and F. G. A. Stone, *J. Chem. Soc., Dalton Trans.*, 1987, 81.
5 M. J. Attfield, J. A. K. Howard, A. N. de M. Jelfs, C. M. Nunn, and F. G. A. Stone, *J. Chem. Soc., Dalton Trans.*, 1987, 2219.
6 M. Green, J. A. K. Howard, A. P. James, A. N. de M. Jelfs, C. M. Nunn, and F. G. A. Stone, *J. Chem. Soc., Dalton Trans.*, 1986, 1697; E. Delgado, L. J. Farrugia, J. Hein, J. C. Jeffery, A. L. Ratermann, and F. G. A. Stone, *ibid.*, 1987, 1191.
7 D. M. P. Mingos, M. I. Forsyth, and A. J. Welch, *J. Chem. Soc., Dalton Trans.*, 1978, 1363.
8 M. Green, J. A. K. Howard, A. P. James, A N. de M. Jelfs, C. M. Nunn, and F. G. A. Stone, *J. Chem. Soc., Chem. Commun.*, 1985, 1778.
9 J. C. Jeffery, J. C. V. Laurie, H. Razay, and F. G. A. Stone, *J. Chem. Soc., Dalton Trans.*, 1984, 1563; J. C. Jeffery, I. Moore, and F. G. A. Stone, *ibid.*, p. 1571; J. C. Jeffery, I. Moore, H. Razay, and F. G. A. Stone, *ibid.*, p. 1581.
10 J. A. Abad, E. Delgado, M. E. Garcia, M. J. Grosse-Ophoff, I. J. Hart, J. C. Jeffery, M. S. Simmons, and F. G. A. Stone, *J. Chem. Soc., Dalton Trans.*, 1987, 41 and refs. therein.
11 G. M. Sheldrick, SHELXTL programs for use with the Nicolet *X*-ray system, University of Cambridge, 1976; updated Göttingen, 1981.
12 'International Tables for *X*-Ray Crystallography,' Kynoch Press, Birmingham, 1974, vol. 4.

Received 19*th December* 1986; *Paper* 6/2443